UAV-Based Atmospheric Tomography

Anthony Finn and Stephen Franklin

Defence and Systems Institute, University of South Australia, Mawson Lakes, SA 5095, Australia

ABSTRACT

A novel technique for remotely monitoring the near-surface air temperature and wind fields based on measurements of the Doppler shift in frequency exhibited as a result of the varying propagation delays between an unmanned aerial vehicle UAV and different acoustic ground receivers is presented. The technique measures the onboard spectrum of sound signals emitted by the engine of an UAV, transmits them to the ground using high bandwidth radio communications and compares them to the Doppler shifted spectra received over propagation paths to several ground-based acoustic receivers. The data are then converted into effective sound speed values using tomographic techniques to reconstruct a two-dimensional grid of spatially varying atmospheric temperature and wind fields.

INTRODUCTION

Tomography is widely used in physics, medicine, and the remote sensing of different media. There are a number of advantages of tomographic observations compared with conventional atmospheric soundings as it enables one to reconstruct 'slices' through the atmosphere of the temperature and wind velocity profiles, and to monitor their evolution in time and space. It is then possible to provide information on the representativeness of point measurements and the homogeneity of atmospheric observations. These fields are important in many practical applications such as boundary layer meteorology, theories of turbulence, wave propagation through a turbulent atmosphere, etc.

If we assume that the UAV is propeller-driven, flying level at constant altitude and sub-sonic airspeed and that accurate navigation data is available, we may assume that the acoustic signal emitted by the UAV consists of one or more sets of harmonic tones superimposed on a broadband random component [1]. The frequency of the narrow-band tone received on the ground will change with time due to the acoustic Doppler Effect.

If the source spectrum is recorded onboard the UAV and accurately time-stamped using a GPS receiver also onboard the UAV it may then be transmitted, together with the UAV's navigation data, to the ground in real time using a radio link. This onboard spectrum can then be compared to the received one observed at the same epochs (again accurately time-stamped using GPS receivers) and determination made of the acoustic propagation delay between the UAV and the ground receiver. If multiple receivers are located on the ground such that they and the UAV's flight trajectory form a single plane, from the range and range-rate information pertinent to the geometry, time travel data along multiple intersecting propagation paths passing through the atmosphere can be determined. Using a suitable inversion procedure, this then allows the reconstruction of a vertical cross-section of the atmospheric profile through which the rays pass in terms of derived, spatially averaged physical parameters such as effective speed of sound, temperature and wind vectors.

There are a number of advantages for this technique when compared to conventional remote monitoring techniques. First, it has advantages in comparison to the point observations of the temperature and wind velocity fields made by traditional techniques (e.g. sonic anemometers) as these devices have inertia, can be affected by radiation, and can dis-turb the temperature and wind velocity fields [2]. Second, the technique requires fewer sensors or transmitters per unit of data (or area) than conventional meteorological devices or schemes that use time difference of arrival techniques to parasitically observe sound sources such as birds, meteors, or commercial aircraft. Furthermore, the trajectories described by the UAV are under user direction so the observation paths of the rays are therefore controllable.

Third, as the aircraft has no pilot and it can be made small (wingspan ~3m) with low kinetic energy so that it may be safely flown at any altitude from a few metres to several kilometres, in dangerous environments such as near hurricanes, cyclones, volcanoes, bush fire fronts, etc, and can fly for long periods. Depending upon the number and density of the ground receivers, the tomographic profiles can then be reconstructed for different regions of the atmosphere: the surface layer, which extends a few metres above the ground (although a propeller-driven aircraft flying so close to the ground may well disturb the atmosphere under observation); the boundary layer, which extends up to heights of a few hundred metres; or – subject to the performance envelope of the UAV – even up to heights of several kilometres. Furthermore, if 2-D arrays of ground sensors and prescribed UAV paths are suitably combined, full 3-D volumetric profiles may be reconstructed and monitored over time.

Fourth, one of the main issues in outdoor acoustic tomography – the formulation of robust and accurate reconstructions of the temperature and wind-velocity fields from a spatially limited set of observations – is overcome as the resolution of the reconstruction of the atmospheric profiles is governed predominantly by the number and spacing of receivers and the duration of the observed spectra relative to the sampling frequency.

Finally, if a rotary wing UAV is used in place of a fixed-wing aircraft, or multiple UAVs are flown simultaneously, the ground receivers may then be placed on moving vehicles (as the dominant acoustic UAV spectrum is higher than that of the ground vehicle it is still readily distinguishable at useful ranges). The entire system is then mobile and able to reconstruct substantially larger or much more complex profiles.

The technique is also extensible to other propagation media and vehicles (e.g. unmanned underwater vehicles) if, rather than transmitting the data in real time via radio frequencies, it is accurately time-stamped and saved for later post-processing. In fact, given the relative simplicity and likely low cost of the ground receiving equipment, the prospect of

an unmanned vehicle deploying (and in the case of an under-water vehicle retrieving) the ground sensor segment is a realistic future consideration.

TRAVEL TIME TOMOGRAPHY FROM UAVS

If we assume a UAV is moving at a velocity, v, relative to a ground receiver such that an angle, θ, is formed between the directions of the UAV's velocity vector and the acoustic propagation path to the ground receiver and that the transmitted spectrum is represented by a dominant frequency component, f_{UAV}, the frequency of the signal received by an acoustic sensor on the ground, f_R, may be given by

$$f_R = f_{UAV} \left[\frac{1 - \left(\frac{v}{c}\right)\cos\theta}{\sqrt{1 - \frac{v^2}{c^2}}} \right]$$

If we ensure that v is significantly less than the speed of sound in air, c, we may approximate the above equation such that the longitudinal Doppler Effect dominates the transverse effect. We may therefore make the assumption that $f_R = f_{UAV}$ $[1 - (v/c)\cos\theta]$. If the range vector from UAV to receiver, $\tilde{r} = \tilde{x}_R - \tilde{x}_{UAV}$, the range, $r = |\tilde{r}|$, and the UAV speed, $v = |\dot{\tilde{x}}|_{UAV}$ then $\cos\theta = \frac{\tilde{r}.\dot{\tilde{x}}_{UAV}}{rv}$ and the Doppler-shifted frequency observed at the receiver is

$$f_R = f_{UAV} + \frac{f_{UAV}}{c}\left[\frac{(x_R - x_{UAV})\dot{x}_{UAV} + (y_R - y_{UAV})\dot{y}_{UAV} + (z_R - z_{UAV})\dot{z}_{UAV}}{\sqrt{(x_R - x_{UAV})^2 + (y_R - y_{UAV})^2 + (z_R - z_{UAV})^2}}\right]$$

$$\Delta t = \frac{f_R - f_{UAV}}{f_{UAV}}\left[\frac{(x_R - x_{UAV})^2 + (y_R - y_{UAV})^2 + (z_R - z_{UAV})^2}{(x_R - x_{UAV})\dot{x}_{UAV} + (y_R - y_{UAV})\dot{y}_{UAV} + (z_R - z_{UAV})\dot{z}_{UAV}}\right]$$

Although local wind conditions at the UAV will vary as a function of time and hence its velocity and the received Doppler will not be constant, if the sample interval is short (~1sec) the UAV velocities and Doppler shifted frequency may be assumed constant over the sample period. The quantities $f_R, f_{UAV}, x_R, y_R, z_R, \dot{x}_R$ and $\dot{z}_R$ are therefore known because they are either observed directly by the receiver on the ground or observed by sensors onboard the UAV which may be transmitted to the ground via radio in real time, leaving the acoustic propagation delay, Δt, as the only unknown.

An alternative approach, similar to that used to determine ego-location from the Transit satellite constellation, is to derive an accurate 1Hz signal from a GPS receiver and 'pulse' or modulate the throttle control of the UAV for fixed periods. If the frequency transmitted by the UAV, f_{UAV}, over the period of throttle modulation, $t_2 - t_1$, is constant it will be received at a frequency, f_R, at the ground receiver between $t_1+\Delta t_1$ and $t_2+\Delta t_2$. If the received signal is then differenced with a (digital) ground reference signal, f_G, and the number of 'beats', D, produced counted during the integration period $D = \int_{t_1+\Delta t_1}^{t_2+\Delta t_2}(f_G - f_R)dt$. As the propagation takes place in a non-dispersive medium, the number of cycles received between $t_1+\Delta t_1$ and $t_2+\Delta t_2$ is the same as that transmitted by the UAV between t_2 and t_1, so

$$D = \int_{t_1+\Delta t_1}^{t_2+\Delta t_2} f_G dt - \int_{t_1}^{t_2} f_{UAV} dt$$

$$= (f_G - f_{UAV})(t_2 - t_1) + \frac{f_G}{c}(r_2 - r_1)$$

Furthermore, as we have assumed small Mach numbers and the acoustic travel time between the UAV and the ground

receiver may be expressed as $\Delta t = \int_{ray}\frac{dl}{c_{eff}}$ (where dl is the element of the arc along the propagation path), for short integration periods

$$\Delta t \approx \frac{(D - (f_G - f_{UAV})(t_2 - t_1))(r_2 + r_1)}{2f_{UAV}(r_2 - r_1)}$$

If we once again transmit the spectrum recorded onboard the UAV to the receivers and use it as the ground reference signal (i.e. $f_G = f_{UAV}$) we then have $D = \frac{f_{UAV}}{c}(r_2 - r_1)$, or

$$\Delta t \approx \frac{D(r_2 + r_1)}{2f_{UAV}(r_2 - r_1)}$$

However we derive Δt we may now divide the plane described by the array of receivers on the ground and the flight trajectory of the UAV into a finite grid of cells such that each cell is crossed by multiple rays passing between the UAV at different epochs and each of the receivers in the array. If we define c_j as the speed of sound (or slowness $s_j = 1/c_j$) in grid cell j and l_{ij} is the length of ray i in cell j, we may now use (J is the total number of rays and L_i is the length of the ith ray)

$$\Delta t_i = \sum_{j=1}^{J}\frac{l_{ij}}{c_j} = \sum_{j=1}^{J}l_{ij}s_j$$

As $c = c_L + \tilde{V}.\tilde{r}$ represents the effective speed of sound with the coupled influence of the virtual acoustic temperature, T, and the wind vector, V, where $c_L = \sqrt{\gamma R_a T}$ is Laplace's

speed of sound, $\gamma = 1.4$ and R_a is the gas constant for air. Re-writing $T = T^0 + T^*$ and $\tilde{V} = \tilde{V}^0 + \tilde{V}^*$ [2], where T^0 and V^0 represent the mean values within the tomographic area of the

temperature and wind, and T^* and V^* their fluctuating components, we have

$$\Delta t_i = \frac{L_i}{c_L}\left(1 - \frac{V_x^0 Cos\theta_i + V_x^0 Sin\theta_i}{c_L}\right) - \frac{1}{c_L}\int_{L_i}\left[\frac{T^*}{2T^0} + \frac{V_x^* Cos\theta}{c_L} + \frac{V_y^* Sin\theta}{c_L}\right]dl$$

Starting with an initial estimate of the slowness values derived from a back-projection of observed acoustic time delays – or from data observed at each of the ground receivers and onboard the UAV and interpolating – we may now apply a least squares adjustment to recursively improve our estimate of the cellular values for the speed of sound using techniques such as Simultaneous Iterative Reconstruction Techniques (SIRT) [3] or those based on Radial Basis Functions [4]. Assumptions regarding horizontal stratification of the atmosphere (such as the absence of large velocity and temperature gradients) will simplify the tomographic reconstruction.

SIGNAL PROCESSING CONSIDERATIONS

In a previous experiment [5] a UAV was positioned just above the ground at a distance 10m from a microphone. The engine of the UAV was then run at full speed (5,700rpm) and the output recorded at a sample rate of 44.1kHz. A time-frequency signal analysis of the recorded data showed strong narrowband tones superimposed onto a broadband random component, with almost all of the narrowband energy below 2kHz. In order to examine this signature more closely the recorded data were then down sampled by a factor of 10 prior to Fourier transformation. The data were processed in over-lapping blocks, each containing 2048 samples, with 50% overlap between two consecutive blocks. A 4096-point fast Fourier transform (FFT) with a Hanning window was then used to compute the spectrum. The spectra of every 3 consecutive data blocks were then averaged to allow a time-frequency analysis of the first 40 harmonics.

It was noted that the frequency and amplitude of each harmonic varied over time, but that over periods of 5sec any variations were linear. Normalising the frequency by its harmonic number produced almost identical results. This is important as some harmonics may not be observable by the ground receivers due to wind noise on the microphones and hence may be used as a means of determining f_R. The mean value of the normalised frequency, f_{UAV}, was 46.9Hz, with 1σ standard deviation (normalised by harmonic number) of 0.46Hz. A more detailed analysis indicated a linear trend in the temporal variation of the frequency of each harmonic (it is assumed this was the effect of the engine warming up) and removal of this trend reduced σ to approximately 0.18Hz. A simple linear extrapolation of this 'calibration' suggests that the error in f_{UAV} will be < 0.003Hz (for an FFT size of 2^{18}), although in reality load changes due to turbulence and other 'mechanical' effects are likely to broaden the spectral line. Given the positional and velocity accuracy of even stand alone GPS ($\sim$10m and 0.2m/s, respectively), therefore, it is errors in f_R that will be the dominant factor in the technique's accuracy. Carrier phase differential GPS provides several orders of magnitude improvement over this.

The UAV selected for this trial is able to travel at speeds of between 18-32 m/s, at altitudes of around 25m to 6km and has a wingspan of 2.9m, an endurance of $\sim$40hours, and can

carry a payload of $\sim$5kg and has also flown in a Category I cyclone [6]. The same equipment and techniques employed above were used to record the output from a microphone when the UAV was flown overhead, except that each data block consisted of 1024 samples and the FFT size was 2048 points. As the harmonic lines were clearly visible in each of the spectrograms derived from the UAV transits they were used as the detection criterion and, based on the average value of the UAV speed, the detection ranges were estimated to be in excess of 1.4km. Using these working assumptions, we may estimate the 'field of view' of each ground sensor to be $\sim$3km and may place an array of sensors over this baseline.
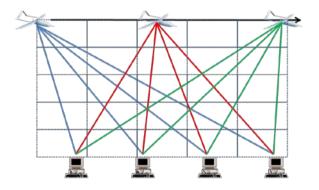

Figure 1: Graphical Depiction of UAV-Based Tomography Concept

If we use a 24 bit ADC at a sample rate of 44.1kHz we must store and transmit $\sim$1Mbit/s, which even without the overhead of compression is well within the capabilities of 802.11g/n and modern flash memory; the navigation and timing data even at 10-20Hz will constitute only a very small overhead to this. Using commercially available 802.11g/n amplifiers this data may then be transmitted reliably over ranges of up to 5km, which is beyond the likely acoustic detection range of the ground sensors.

In order to maximise the accuracy with which we are able to determine Δt we will want to increase the size of the FFT sample of f_R, but are constrained by the potential lack of linearity in the UAV's signature and its degree of motion. On the basis of the sampled data in [5], samples of up to 10sec could be used without significantly violating the assumption of constant frequency over the sample size. A 2^{18} point FFT (i.e. 2^{17} samples per block) represents $\sim$3 seconds of data, although as the UAV could move almost 100m in this time this may effectively 'smear' the resultant observations. The computing requirements of such an FFT are well within the capabilities of the modern portable computers, taking only about 30ms in MATLAB^{TM} on a standard PC. With the use of zero-padding (appending a string of zeros to the time series data to improve the frequency resolution), we should be able to achieve a frequency resolution of $\sim$0.01Hz or, as the error in

the reconstruction of the wind vector $\Delta v \sim \frac{c^2 \Delta t}{r}$ [7], $\Delta v \sim$ 0.5m/s. An alternative is to use $\Delta t \approx \frac{D(r_2 + r_1)}{2 f_{UAV}(r_2 - r_1)}$, for which the error in $\Delta t \sim 0.3D$ for r ~ 1.5km. Integrating over the same 3 sec sample period to resolve D to 0.01 cycles (i.e. ~ 4 deg) would provide similar performance. However, fluctuations in the in the frequency of the of the acoustic signature of the UAV over the UAV duration in the presence of turbulence will likely broaden the spectral lines and probably limit the achievable resolution beyond that obtainable from the maximum practical FFT length.

Over the transit time experienced by a single receiver 3 sec samples represent about 30 tomographic observations over a period of about 94sec (or 55 observations if the UAV travels at 18m/s). As we only have 3 unknowns, T^*, V_x^* and V_y^*, if we deploy a similar number of sensors on the ground (i.e. every 30m in our linear array) we are presented with between $30N$ and $55N$ observations of the intervening atmosphere for a single transit ($N \geq 4$ is the number of ground sensors). We also have the possibility that we could significantly improve the spatial resolution by flying multiple transits over the receiver array, although this would time-average the reconstruction. Alternatively, we can reduce the size of the FFT (say to 2^{16} – i.e. 2^{15} samples per block) and correspondingly increase the number of observations. Even if we limit ourselves to a basic uniform grid, the cell size will then have linear dimension of ~25m. The basic concept is depicted graphically in Figure 1.

In addition to the narrowband tones, the UAV signature observed on the ground will contain broadband acoustic energy, which will arrive at each ground sensor via both the direct and ground reflected path (multi-path). Furthermore, as it contains strong harmonically related tones any correlation function will contain ambiguous peaks. However, as we have the full time series and accurate navigation data from the UAV, using the same techniques employed by [5], we can use this to calculate the maximum multipath delay,

$h_r / c \cong 7ms$ (where h_r is the height of the ground receiver), and hence the direct path signal. The experimental results of [5] also indicate that these broadband correlation techniques lead to improvements in the detection range of the UAV by a factor of two; or approximately $60N$ tomographic observations.

In addition to any self noise signature observed by sensors onboard the UAV, however, there will also be noise induced by the effects of air flow over the platform. Flow noise is broadband in nature and will likely contribute 5-10dB to the overall noise component [7]. This may diminish our capacity to exploit the detection based on time-series cross-correlation. As the dominant noise remains that of the highly correlated narrowband spectral lines that originate from the propulsion engine and correspond to the harmonic series of the cylinder firing rate (and the flow noise is uncorrelated), we can once again exploit the processing techniques employed by [5] to achieve maximal range detection.

As local wind conditions may vary the velocity of a small UAV over intervals even as short as 1 sec, it may be necessary to rely upon state space data ($x_R, y_R, z_R, \dot{x}_R, \dot{x}_R$ and $\dot{z}_R$) derived by averaging it over the integration period rather than a single instantaneous value. GPS and inertial measurement units which provide position and velocity data at 10-20Hz are

readily available and are required onboard the UAV for autonomous flight anyway.

Preliminary Results

In order to improve our understanding of the likely performance envelope of the technique a series of numerical simulations was conducted. Figure 3 (image on the left) shows the temperature profile (in degrees Celcius) used to generate the acoustic observations at an array of ground receivers. The vertical axis is the distance from the UAV (i.e. 0m equates to an altitude of 1000m and 1000m an altitude of 0m). In this example, the ground receivers were deployed over a 12km baseline and were separated by a distance of 100m. Their detection range was modelled as 2.3km. The effects of observed variation in the UAV and ground receiver spectra are modelled separately, but both as 0.2Hz (1σ) random variation on the blade rate frequency of 46.9Hz. The GPS positional and velocity errors were modelled as 10m and 0.1m/s, respectively. The UAV's horizontal velocity was 32m/s (its vertical velocity was assumed to be zero). The FFT size was 4096 and the sampling rate 50kHz. The acoustic signal observed by one of the ground receivers as a result of the passage of the UAV is shown in Figure 2.
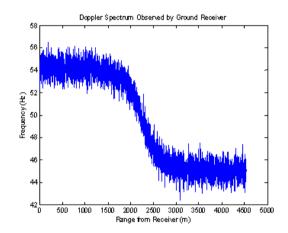

Figure 2: Acoustic Doppler Profile for the Passage of the UAV

The region was then divided into a uniform 50 x 50 segment grid and the tomographic inversion then solved using a constrained, weighted, cumulative least squares adjustment. The observations were first pre-filtered by excluding 'noisy' observations (i.e. greater than 3σ variation from the expected and then their contribution to the least squares adjustment weighted in accordance with the number of rays passing through each cell and the length of ray in the tomographic grid. The adjustment was then constrained by heavily weighting the temperatures at each of the ground receivers to the temperatures known to exist in each of these cells (i.e. it was assumed that each ground receiver was able to measure temperature). Each pixel was also constrained by weighting it as a mean of its neighbours. The resulting inversion is shown in Figure 3. Wind profiles have not been reconstructed at this stage.
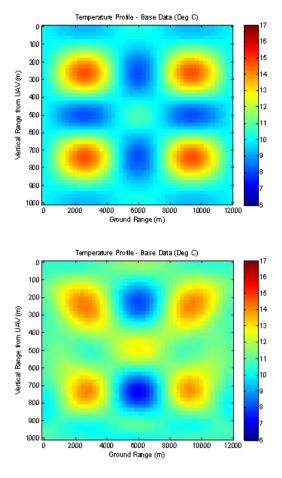
Figure 3: Temperature Profiles for 12km array and UAV at 1km Altitude. The reconstructed profile is on the right

CONCLUSIONS

The main contribution of this paper is the description of a novel technique for remotely monitoring the atmospheric temperature and wind fields based on observations of the passage of a UAV. A simulation and basic error analysis are also performed, which provides an estimate of the performance that could be anticipated in the real world. The technique would potentially permit observations to be made at a range of altitudes and in complex or near hazardous regions such as hurricanes, fire fronts, and volcanoes. Aside from the cost of the UAV, which can be hired, the equipment is expected to be largely inexpensive and commercially available.

REFERENCES

[1] B.G. Ferguson & K.W. Lo, Turbo-prop and rotary-wing aircraft flight parameter estimation using both narrowband and broadband passive acoustic signal processing methods, J. Acoustic Society America, Vol. 108, No. 4, October 2000

[2] V.E. Ostashev et al, Recent progress in acoustic tomography of the atmosphere, Proc. 14th International Symposium for the Advancement of Boundary Layer Remote Sensing, IOP Conference Series (Earth & Environmental Science) IOP Publishing, 2008

[3] A. C. Kak &M. Slaney, *Principles of Computerized Tomographic Imaging,* Society of Industrial and Applied Mathematics, 2001

[4] T. Wiens & P. Behrens, Turbulent flow sensing using acoustic tomography, Proceedings of Innovations in practical Noise Control 2009, Ottawa, Canada, August 2009

[5] K.W. Lo & B.G. Ferguson, Tactical unmanned aerial vehicle localisation using ground-based acoustic sensors, Proceedings Intelligent Sensor, Sensor Networks & Information Processing Conference 2004, Melbourne, December 2004

[6] G. Tyrrell, AAI/Aerosonde Corporation, Private Communication, 2006

[7] B.G. Ferguson, K.W. Lo & R. Wyber, Acoustic sensing of direct and indirect weapon fire, Proceedings Intelligent Sensor, Sensor Networks & Information Processing Conference 2007, Melbourne, December 2007

[8] V.E. Ostashev, A.G. Voronovich & D.K. Wilson, Acoustic tomography of the atmosphere, Proc. IEEE International Geoscience & Remote Sensing Symposium, 2000